AIAA Meeting Papers on Disc, July 1996
A9636997, N00014-95-1-0163, AIAA Paper 96-2759

# Fuzzy logic control of reheat buzz

**S. Menon**
*Georgia Inst. of Technology, Atlanta*

**Y. Sun**
*Georgia Inst. of Technology, Atlanta*

**AIAA, ASME, SAE, and ASEE, Joint Propulsion Conference and Exhibit, 32nd, Lake Buena Vista, FL, July 1-3, 1996**

A fuzzy logic based feedback controller has been developed to suppress combustion instability in a reheat buzz device which is a simplified approximation to an afterburner in an engine nozzle. The results clearly demonstrate that the fuzzy controller is as effective as deterministic controllers. When the control goal is within the fuzzy rule base, the controller is successful on the first attempt. When the control goal is outside the rule base, a simple redefinition of the rule base is sufficient to achieve control. Comparison with earlier experimental and numerical results clearly show that the present calculations agree quite well with data. (Author)

# Fuzzy Logic Control of Reheat Buzz

S. Menon* and Y. Sun +
School of Aerospace Engineering
Georgia Institute of Technology
Atlanta, Georgia 30332-0150

## Abstract

A fuzzy logic based feedback controller has been developed to suppress combustion instability in a reheat buzz device which is a simplified approximation to an afterburner in an engine nozzle. The results clearly demonstrate that the fuzzy controller is as effective as deterministic controllers. When the control goal is within the fuzzy rule base the controller is successful on the first attempt. When the control goal is outside the rule base, a simple redefinition of the rule base is sufficient to achieve control. Comparison with earlier experimental and numerical results clearly show that the present calculations agree quite well with data.

## 1. Introduction

In jet engine afterburners, a low frequency combustion instability, often called reheat buzz, has been observed. Physically, this phenomenon is due to the coupling between the propagating pressure waves and the unsteady heat release and manifests itself as a low frequency pressure oscillation. When the heat release is in-phase with the pressure (acoustic) waves (called the Rayleigh criterion), the pressure waves can grow in amplitude. This instability has also been generated in laboratory rigs. An extensive research study at Cambridge University (e.g., Bloxsidge et al., 1988a; Dowling, 1989; Langhorne, 1988) investigated this phenomenon using both experimental and theoretical studies and demonstrated that this instability is related to longitudinal, long-wavelength pressure wave. Further experimental studies were then carried out to determine a methodology to control this instability. Various active control methods were investigated, such as: unsteady inlet flow modification (Lang et al., 1987), acoustic forcing (Bloxsidge et al., 1987, 1988b) and unsteady secondary fuel injection (Langhorne and Hooper, 1989; Langhorne et al., 1989). Although, all these methods appeared to be successful, only secondary fuel injection was deemed to be practical due to the hostile environment of the engine nozzle (Langhorne et al., 1989).

Other combustion systems, such as ramjets and dump combustors (in gas turbine engines) also exhibit this low frequency, large-amplitude pressure oscillation (e.g., Schadow et al., 1987; Poinsot et al., 1987a; Yu et al., 1991). These experimental and numerical (e.g., Menon and Jou, 1991) studies revealed that combustion instability in these devices is also due to the coupling between the unsteady heat release and pressure oscillations. However, in dump combustors, the propagation of unsteady vortex structures (due to shedding at the dump plane) at the instability frequency was shown to play a major role in the instability process. Vortex shedding may also play a major role in afterburners due to the presence of flame holders.

Further studies (e.g., Poinsot et al., 1987b; Schadow et al., 1990; Wilson et al, 1995; Gutmark et al., 1995; Menon, 1992a, 1992b, 1995) showed that secondary fuel injection is a practical option for active control in dump combustors, However, attempts using deterministic controllers (e.g., Wilson et al., 1995; Gutmark et al., 1995; Menon, 1995) have had only limited success. In particular, results show that, in flows where the instability is due to a coupled acoustic-convective mode (e.g., Yu et al., 1991; Gutmark et al., 1995; Menon, 1995), the amplitude of the instability frequency is reduced but system instability shifts to a new frequency that is not controlled. This is due to the highly nonlinear interactions between the acoustic waves, vortex motion and unsteady heat release. Therefore, adaptive controllers based on neural network have been investigated. Results show significant promise but the training of the neural net can be considerable. Furthermore, the net must be trained on the actual system, thereby, making *a priori* development of a general purpose control system difficult.

An alternate method that employs fuzzy logic based controller is studied here. Based on past studies (e.g., Kosko, 1992), it appears that the

*Associate Professor, Senior Member AIAA
+Graduate Research Assistant

training required to develop the fuzzy rule base need not be as extensive as for neural nets.

Fuzzy controllers for combustion instability have not yet been investigated. To demonstrate the feasibility of such a controller, a model simulation is carried out in this paper using the reheat buzz device noted above. This device is employed for two major reasons: (a) there is an extensive experimental and numerical data base from past studies with and without active control, and, (b) the instability process is very similar to that occurring in dump combustors. Therefore, it is expected that the demonstration of an active control methodology using this device will lay the groundwork for developing a similar robust strategy for control in dump combustors.

Fuzzy control has been applied in the past to a variety of non-linear systems and has been shown to be as effective as conventional control (Kosko, 1992). Large-scale systems such as textile processing (Kim et al., 1994) and refuse incineration (Ono et al., 1989) plants were successfully controlled using fuzzy algorithms. The fuzzy system can be considered as a real-time system that is implemented in a heuristic and modular manner to achieve the control objectives. The control algorithm attempts to mimic the operator (human) expertise and thus, does not lend itself to be expressed in conventional proportional-integral-derivative (PID) -parameters or differential equations and therefore, must be expressed in situation/action rules. It has been proven by Kosko (1992) that any continuous nonlinear function can be approximated as needed with a finite set of fuzzy variables and rules. The primary benefits of a fuzzy system is that it can be implemented using expert knowledge, thus, providing a higher degree of automation than deterministic controllers.

This paper describes a numerical demonstration of a fuzzy logic based controller for controlling combustion instability in a reheat buzz device.

## 2. Formulation of the Model

The device used by researchers at Cambridge University (e.g., Bloxsidge et al., 1987, 1988a, 1988b; Langhorne, 1988; Dowling, 1989) is employed for the present study. Following earlier numerical studies (Bloxsidge et al., 1988a), a one dimensional model is also used here. This approximation was shown earlier (Bloxsidge et al., 1988a) to be quite accurate for this type of instability.

Figure 1 shows the schematic of the reheat buzz test rig. The device consists of a long duct of circular cross-section of variable length L. Premixed fuel-air mixture enters this duct at $x = 0$ and is ignited at a conical gutter, located at $x = x_g$, that acts like a bluff body to stabilize the flame. More details of experimental device is given elsewhere (e.g., Langhorne, 1988; Langhorne et al., 1989) and therefore, avoided here for brevity.

The baseline numerical model (i.e., without control) is similar to the earlier model (Bloxsidge et al., 1988a). Therefore, the methodology, the governing equations and the symbols used here are similar. However, for completeness, the formulation is repeated here. The governing equations are obtained from the conservation laws with the assumption that the mean flow is essentially one-dimensional and at steady state. Superimposed on this mean flow is a perturbation that is periodic in nature and at a (unknown) frequency (this frequency is determined as a part of the solution).

To model this rig with a 1D model, the device is divided into sections I-IV (see Fig. 1). Section I is the inflow duct, section II is the gutter section that includes the flame holder, section III is the flame zone and section IV is the outflow portion of the duct.

### 2.1 The mean flow

Assuming that the mean flow is steady, inviscid and one-dimensional, the conservation of mass, momentum and energy can be written, respectively as $d\overline{m}/dx = 0, d\overline{F}/dx = 0$ and $d\overline{E}/dx = \overline{q}(x)$, where, $\overline{m}, \overline{F}$ and $\overline{E}$ are defined (in terms of the primitive variables), respectively, as: $\overline{m} = \overline{\rho}\,\overline{u}A, \overline{F} = \left(\overline{p} + \overline{\rho}\,\overline{u}^2\right)A$ and $\overline{E} = \overline{m}\left(C_p\overline{T} + \frac{1}{2}\overline{u}^2\right)$. Here, A is the local area, $\overline{\rho}$ is the mean density, $\overline{p}$ is the mean pressure, $\overline{T}$ is the mean temperature, $\overline{u}$ is the mean axial velocity, $C_p$ is the specific heat at constant pressure and $\overline{q}(x)$ is the mean heat release. These equations are supplemented by the equation of state: $\overline{p} = \overline{\rho}R\overline{T}$ to close the system of equations. Here, R is the gas constant. Once the quantities $\overline{m}, \overline{F}$ and $\overline{E}$ are obtained, all the mean flow properties can be obtained by using

the relations: $\overline{\rho} = \overline{m}/\overline{u}A$, $\overline{T} = (\overline{p}/R\overline{\rho})$, and $p = (\overline{F} - \overline{mu})/A$. The mean velocity is: $\overline{u} = \frac{\gamma\overline{F}}{(\gamma+1)\overline{m}}\left[1-\left(1-\frac{2(\gamma^2-1)\overline{m}\overline{E}}{\gamma^2\overline{F}^2}\right)^{1/2}\right]$, where, $\gamma$ is the ratio of specific heats.

The mean flow equations are solved in each section (I-IV) using appropriate boundary conditions. At the inlet, $x = 0$, the flow Mach number, the fluid density and the temperature are assumed known. Using these conditions, the mean axial velocity at the inlet and the mass flow rate can be determined. With these quantities known at the inlet, all other properties can be determined using the relations given above. Since there is no heat release in the inlet duct section, the inlet conditions specify the mean flow properties in the entire section I.

The fuel injector (gutter) section (section II) is assumed much smaller (in length) than the duct and its influence is modeled in terms of changes in the flow properties due to the change in the duct area. Again, no heat release occurs in this section. To determine the mean flow properties in section II the conservation rules imply: $\overline{m}_{II} = \overline{m}_I, \overline{E}_{II} = \overline{E}_I, \overline{p}_{II}/\overline{\rho}_{II}^{\gamma} = \overline{p}_I/\overline{\rho}_I^{\gamma}$ and $\overline{p}_{II} = \overline{\rho}_{II}R\overline{T}_{II}$. Here, the subscript indicates the appropriate section of interest. To determine the mean flow properties, the above conditions are used in an iterative algorithm. The method involves first guessing the axial velocity in section II, $\overline{u}_{II}$ and then, determining the mean density from the relation: $\overline{\rho}_{II} = \overline{m}_{II}/\overline{u}_{II}A_{II}$, the mean pressure from $\overline{p}_{II} = (\overline{p}_I/\overline{\rho}_I^{\gamma})\overline{\rho}_{II}^{\gamma}$ and the mean temperature from the equation of state. The total energy, $\overline{E}_{II}$ is then estimated. To maintain energy conservation, $\overline{E}_{II} = \overline{E}_I$ must be satisfied. If this condition is not met, the initial guess of the mean axial velocity, $\overline{u}_{II}$ is changed and the iteration continued till the convergence criterion is met.

In section III, combustion and hence, heat release occurs. The flame zone is modeled as a control volume which is assumed long enough that the conditions at the end of section III again can be approximated using 1D. Conservation rules imply that: $\overline{m}_{III} = \overline{m}_{II}, \overline{E}_{III} = \overline{E}_{II} + \overline{Q}_c$, $\overline{p}_{III} = \overline{\rho}_{III}R\overline{T}_{III}, \overline{F}_{III} = \overline{F}_{II} + \overline{p}_{II}(A_{III} - A_{II})$.

Here, $\overline{Q}_c$ is the mean heat release within the volume given by: $\overline{Q}_c = \int_{x_t}^{x_d}\overline{q}(x)dx$. Here, the subscript II (or $g$) indicates the flame holder (gutter) section (i.e., the end of section II) and subscript III (or $d$) indicates the end of section III. Once the properties, $\overline{m}, \overline{F}$ and $\overline{E}$ are determined, then other flow properties (defined in terms of $\overline{m}, \overline{F}$ and $\overline{E}$, see above) can be determined.

Downstream of the flame holder section, section IV is the combustor in which the flow properties can be determined as in Section I except that in this section, mean heat release is assumed to occur.

## 2.2 The Perturbed Flow

In this study (and, as in Bloxsidge et al., 1988a), the flow is assumed to be perturbed by a disturbance so that any instantaneous flow property $\phi$ assumes the form:

$$\phi(x) = \overline{\phi}(x) + \phi'(x,t) = \overline{\phi}(x) + \hat{\phi}(x)e^{i\omega t} \quad (1)$$

Here, the disturbance field is assumed to be periodic in nature at a (as yet unknown) complex frequency, $\omega$, whose real part gives the frequency of oscillation and its imaginary part gives the phase. Also, $\hat{\phi}$ is the amplitude of the perturbation. The mean and the perturbed equations can easily be obtained from the conservation equation. The perturbed relations are:

$$\hat{m} = (\hat{\rho}\overline{u} + \overline{\rho}\hat{u})A \quad (2)$$

$$\hat{F} = (\hat{p} + \hat{\rho}\overline{u}^2 + 2\overline{\rho}\overline{u}\hat{u})A \quad (3)$$

$$\hat{E} = \hat{m}\left(C_p\overline{T} + \frac{1}{2}\overline{u}^2\right)A + \overline{m}\left(C_p\hat{T} + \overline{u}\hat{u}\right)A \quad (4)$$

and

$$\frac{\hat{p}}{\overline{p}} = \frac{\hat{\rho}}{\overline{\rho}} + \frac{\hat{T}}{\overline{T}} \quad (5)$$

The perturbed flow variables are obtained from the relations:

$$\hat{u} = \frac{1/2(\gamma+1)\overline{u}^2\hat{m} - \gamma\overline{u}\hat{F} + (\gamma-1)\hat{E}}{\left(\gamma\overline{p} - \overline{\rho}\overline{u}^2\right)A} \quad (6)$$

$$\hat{\rho} = \frac{\hat{m}}{\overline{u}A} - \frac{\overline{\rho}\hat{u}}{\overline{u}} \quad (7)$$

$$\hat{p} = \frac{\hat{F}}{A} - \overline{\rho}\overline{u}\hat{u} - \frac{\overline{u}\hat{m}}{A} \quad (8)$$

$$\hat{T} = \frac{\hat{E}}{C_p\overline{m}} - \frac{\hat{m}}{\overline{m}}\left(\overline{T} + \frac{\overline{u}^2}{2C_p}\right) - \frac{\overline{u}\hat{u}}{C_p} \quad (9)$$

The perturbed equations are solved in each section subject to appropriate boundary conditions. Since the disturbance is unsteady, the 1D unsteady inviscid equations are used. Therefore, the perturbed field have to be solved using a difference form. For example, the 1D unsteady conservation of mass is:

$$\frac{\partial\rho A}{\partial t} + \frac{\partial(\rho u A)}{\partial x} = 0 \quad (10)$$

Using the definitions: $\rho(x,t) = \overline{\rho}(x) + \hat{\rho}e^{i\omega t}$, $u(x,t) = \overline{u}(x) + \hat{u}e^{i\omega t}$, and noting that the area A is constant, we obtain:

$$\frac{d\hat{m}}{dx} = -i\omega\hat{\rho}A \quad (11)$$

Similarly, the conservation of momentum and energy reduces to

$$\frac{d\hat{F}}{dx} = -i\omega\hat{m} \quad (12)$$

and

$$\frac{d\hat{E}}{dx} = \hat{q} - i\omega[\hat{\rho}(C_v\overline{T} + \frac{1}{2}\overline{u}^2) + \overline{\rho}(C_v\hat{T} + \overline{u}\hat{u})]A \quad (13)$$

These equations are solved subject to appropriate boundary conditions. At the inflow, $x = 0$ (section I), the inflow conditions are: $\hat{\rho}(0) = \hat{p}(0)\overline{\rho}(0)/\gamma\overline{p}(0)$, $\hat{p}(0) = 1$, and $\hat{u}(0) = -\hat{\rho}(0)\overline{u}(0)/\overline{\rho}(0)$. The outflow condition at $x = L$ (section IV) is $\hat{p}(L) = 0$.

In section I, the perturbed equations are solved using finite differences subject to the specified boundary conditions. The resolution used is sufficiently small to ensure grid independent result.

In section II, the presence of the fuel injector is reflected as a change in the effective area. Therefore, as for the mean flow, the perturbed fields in section II are determined from the fields in section I from the relations: $\hat{m}_{II} = \hat{m}_I$, $\hat{p}_{II}/\overline{p}_{II} - \gamma\hat{\rho}_{II}/\overline{\rho}_{II} = \hat{p}_I/\overline{p}_I - \gamma\hat{\rho}_I/\overline{\rho}_I$, $\hat{E}_{II} = \hat{E}_I$ and $\hat{p}_{II} = \hat{\rho}_{II}R\overline{T}_{II} + \overline{\rho}_{II}R\hat{T}_{II}$. Again, an iterative method is used to solve these equations. This method follows the approach used to determine the mean flow.

In section III, the governing equations for the perturbed fields are (Bloxsidge et al., 1988a):

$$\hat{m}_g - \hat{m}_d = \left(\overline{\rho}_g - \overline{\rho}_d\right)\frac{d\hat{\alpha}_1}{dt}$$

$$\hat{F}_g - \hat{F}_d + \hat{p}_g(A_d - A_g) = \left(\overline{\rho}_g\overline{u}_g - \overline{\rho}_d\overline{u}_d\right)\frac{d\hat{\alpha}_1}{dt} + i\omega[(\hat{\rho}_g\overline{u}_g + \overline{\rho}_g\hat{u}_g)\overline{\alpha}_1 + (\hat{\rho}_d\overline{u}_d + \overline{\rho}_d\hat{u}_d)\overline{\alpha}_2] \quad (15)$$

$$\hat{E}_g - \hat{E}_d + \hat{Q}_c = \left[\overline{\rho}_g\left(C_v\overline{T}_g + \frac{1}{2}\overline{u}_g^2\right) - \overline{\rho}_d\left(C_v\overline{T}_d + \frac{1}{2}\overline{u}_d^2\right)\right]\frac{d\hat{\alpha}_1}{dt} + i\omega\overline{\alpha}_1\left[\hat{\rho}_g\left(C_v\overline{T}_g + \frac{1}{2}\overline{u}_g^2\right) + \overline{\rho}_g\left(C_v\hat{T}_g + \overline{u}_g\hat{u}_g\right)\right] + \overline{\alpha}_2\left[\hat{\rho}_d\left(C_v\overline{T}_d + \frac{1}{2}\overline{u}_d^2\right) + \overline{\rho}_d\left(C_v\hat{T}_d + \overline{u}_d\hat{u}_d\right)\right] \quad (16)$$

and

$$\hat{p}_d = \hat{\rho}_d R\overline{T}_d + \overline{\rho}_d R\hat{T}_d. \quad (17)$$

The above relations account for the unsteady changes in the flame zone due to combustion (see Bloxsidge et al., 1988a, for more details). Here, $\alpha_1$ and $\alpha_2$ represents, respectively, the volume of unburned gas within the control volume and the volume occupied by the hot gas within the same control volume. Conservation rules are applied to the total volume $\alpha_1 + \alpha_2$ (which is a constant). Further details are given in Bloxsidge et al. (1988a). Briefly, the parameters

$\overline{\alpha}_1$ and $\overline{\alpha}_2$ are determined by assuming that, on the average, the flame sheet takes the shape of a truncated cone of axial length $(x_d - x_g)$. Thus,

$\overline{\alpha}_1 = \frac{1}{3}\pi(x_d - x_g)(2r_d^2 - r_d r_g - r_g^2)$, and

$\overline{\alpha}_2 = \frac{1}{3}\pi(x_d - x_g)(r_d^2 + r_d r_g + r_g^2)$. Here, $r_d$ and $r_d$ are respectively, the radius of the gutter lip and the downstream duct. The time derivative term $d\hat{\alpha}_1/dt$ is determined using mass conservation in $\alpha_1$ and the rate of heat release at the flame front. The resulting relation is: $\frac{d\hat{\alpha}_1}{dt} = \frac{\hat{m}_g}{\overline{\rho}_g} - \frac{\overline{m}_g \hat{Q}_c}{\overline{\rho}_g \overline{Q}_c} - \frac{i\omega\hat{\rho}_g\overline{\alpha}_1}{\overline{\rho}_g}$. These relations are used in Eqns (14-16) to close system of equations.

To solve these equations in section III, a finite difference scheme is again employed. The major input to the equations in section III is the form of the heat release perturbation. In Bloxsidge et al. (1988a), various flame models were devised to match the experimental data. In the present study, a similar approach is carried out. For example, the mean and the perturbation forms of heat release per unit duct length are chosen (for a given operating condition), respectively, as:

$$\overline{q}(x) = k(x - x_g) \text{ for } x > x_g \qquad (18a)$$

(and zero elsewhere)

$$\hat{q}(x) = \overline{q}(x)\frac{\hat{u}_g}{iSt\overline{u}_g}e^{i\omega\tau(x)} \qquad (18b)$$

Here, $\tau(x) = (x - x_g)/\overline{u}_g$ is a time scale and St is the local Strouhal number defined as $St = 2\pi r_g \omega/\overline{u}_g$. Eqns. (18a-b) are obtained by noting that the heat release is proportional to light emission in the flame zone and by using the experimental data to find a best fit. Experimental data gives: $k = 0.66 MW/m^2$ in Eq. (18a). Further details are given in Bloxsidge et al. (1988a). Note that, for other operating conditions, the flame models have to be modified to match with appropriate data.

The perturbation field in section IV is determined as in section I expect for the presence of the unsteady heat release term.
Solution of the perturbation field also requires the value of the complex frequency $\omega$. Previously (Bloxsidge et al., 1988a), the frequency was determined by solving an eigenvalue problem. Here, the frequency is determined by an iterative method, whereby, the frequency is initially guessed and the perturbation field determined in all the sections. The criteria for convergence is to ensure that the boundary condition at the end of section IV, $\hat{p}(L) = 0$, is satisfied. Iteration is continued till this condition is satisfied to required accuracy.

## 3. The Fuzzy Logic Algorithm

The goal of a fuzzy "response" (i.e., controller) to a fuzzy "signal" (i.e., sensor response) is to provide an output that will "approximate" an optimal response to drive the nonlinear system to the pre-specified set point. To develop the fuzzy controller, a set of rules must be devised based on experiments and/or operator experience. A fuzzy rule so devised relates fuzzy concepts in the form a conditional statement (Kosko, 1992; Driankov et al., 1993). For example, "*IF X is A, THEN Y is B*" is a conditional statement in which A and B are fuzzy sets (here identified as sensor signal and control output, respectively). The fuzzy sets A and B must be defined before the controller can be implemented.

To build a fuzzy control system, three steps have be carried out. The first step involves identification of the principal variables (X and Y). For example, in the present study, the variable X is identified as the pressure sensor signal (amplitude and/or phase) and the variable Y is identified as the controlled secondary fuel injection (flow rate and/or phase). The second step is to define the fuzzy sets A and B associated with the variables X and Y. The choice of these sets are based on preliminary experiments with *open loop* control to determine the system response to the controller. In addition, operator experience can be used to define these fuzzy sets. Here, using the pressure amplitude as the sensor variable (X) and secondary fuel injection phase or flow rate as the output (Y), we chose the elements of the fuzzy sets A and B. Thus, the fuzzy set A could be chosen as {*too low, low, JUST RIGHT, medium, large*} to define the pressure oscillation amplitude and the set B could be chosen for secondary fuel injection PHASE (relative to the phase of pressure perturbation) as {*positive max, positive medium, ZERO, negative medium, negative max*} or for the secondary fuel injection FLOW RATE as {*medium, low, none, low, medium*}. As noted here, the fuzzy sets can be chosen so that the controller will not react or respond during proper operation (i.e., when X is *JUST RIGHT*).

The third step is to define the fuzzy rules that will provide the relationship between the fuzzy rules. A typical set of fuzzy rules could be : "*IF X=X1, THEN Y=Y1; IF X=X2, THEN Y=Y2; IF X=X3, THEN Y=Y3;* etc." where X1-X3 and Y1-Y3 correspond to the values in the sets X and Y. Each rule has a *range* with variable probability of occurrence and looks like *patches* (see Figs 6 and 7, below). Smaller patches (i.e., when the sets A and B contain many members) are more precise and hence, less fuzzy. The specific value of the set, i.e., X1, X2, etc., are considered the centroid of the respective rule. The shape of the patches are chosen from a library of *membership functions*. Various membership functions are available (Kosko, 1992) to define these rules. The particular choices of the membership functions for the present problem are discussed later in section 4.

In a typical application, all the rules are executed *simultaneously* and in *parallel*; however, the outcome is determined by the weighted average. The process of *defuzzification* is then required, whereby, the response is determined by the centroid of the weighted mean. The use of fuzzy patches allow for application of the control even when the input (sensor) is recording a value that belongs to two fuzzy set members. The correct response required from the controller is then determined by the sum of the probabilities for each of the fuzzy set members, and the resulting weighted average.

### 3.1 Fuzzy Logic Control of Reheat Buzz

To apply fuzzy logic to control the instability, the algorithm described above must be specialized, and then, applied in the numerical model. As noted above, open loop control simulations are needed to obtain the experience to device the fuzzy rules. Therefore, a series of simulations were carried out using the pressure amplitude as the sensor and the PHASE of the unsteady injection as the control. Thus, if the pressure perturbation is given as in Eq. (1), the secondary fuel injection flow rate is: $\dot{m}_{sec} = \hat{\dot{m}}_{sec} \exp[i(\omega t + \phi)]$ where, $\phi$ is the phase of the secondary fuel injection and $\hat{\dot{m}}_{sec}$ is the amplitude of the secondary fuel flow rate chosen as: $\hat{\dot{m}}_{sec} = \varepsilon \hat{\dot{m}}_1$ where $\varepsilon$ is a constant pre-specified to be 0.03. Thus, the secondary premixed fuel injected into the system is a small fraction of the primary flow rate. The effect of varying the secondary flow rate has not yet been studied, but the flow rate chosen is consistent with past studies (e.g., Langhorne et al., 1989; Menon, 1995) where it was shown that even a small amount of secondary fuel can effectively control the instability. The location of the secondary fuel injection is chosen (rather arbitrarily) at the beginning of the gutter section (section II - see Fig. 1). Since the addition of the secondary premixed fuel only increases the net flow rate, the flame model does not have to be changed.

For secondary injection, the boundary matching conditions (between sections II and III) have to be modified to reflect the increase in the mass flow rate. With these conditions defined, a series of calculations were carried out by systematically varying the phase $\phi$ to evaluate the behavior of the controller. The sensor location is chosen in section IV (see Fig. 1) and the amplitude of the pressure perturbation at this location is monitored during the simulations.

Results of these studies and studies with the fuzzy controller are discussed in the next section.

## 4. Results of the Study

In this section, the results of the simulations are presented. First, the predictions without any control are compared to the experimental data. This serves to confirm the validity of the present numerical methodology. Subsequently, the secondary injection control is implemented and a series of calculations were carried out (in the *open loop* configuration) to coarsely map the response of the system to changes in the phase of the fuel injection. Using this data, the fuzzy rules were developed and then, the ability of the fuzzy controller to drive the pressure perturbation to a pre-specified set point was evaluated. Comparison with the experimental data (obtained using a deterministic controller) of Langhorne et al. (1989) is also carried out to demonstrate that the fuzzy controller is capable of controlling the pressure oscillation in a very similar manner.

### 4.1 Validation of the model

The numerical model described in section 2 was solved and the results compared to earlier calculations (Bloxsidge et al., 1988a) and experiments (Dowling, 1989; Langhorne, 1988). Various configurations (shown in Table I) were investigated. The frequency and growth rate for the pressure fluctuation in the device obtained in the present study are shown in this table along with the earlier results. Clearly, the present predictions are in good agreement with the past

results. Note that, differences in the test configurations and or conditions resulted in differences in the measured heat release. Therefore, a key input to the numerical model was a "curve" fit to the heat release data. Thus, various flame models (e.g., the established and weak flame models, see Bloxsidge et al., 1988a) were employed to compare with the experiments. Configurations 1, 3-5 were calculated using the established flame model while configuration 2, which was for a lower fuel-to-air ratio, was computed using the weak flame model.

Only representative results are shown (for Configuration 1) since results obtained for other configurations also give similar agreement. Figure 2 shows the mean heat release model used to match with the data. Figures 3a and 3b show respectively, the amplitude and the phase of the pressure perturbation, and, Figs. 4a and 4b show respectively, the amplitude and the phase of the unsteady heat release. The present predictions are compared to the past experimental and numerical data. As seen, the agreement is quite good. These studies serves to validate the present baseline numerical model.

## 4.2 Open Loop Control Simulations

With the baseline model validated for the experimental device, a series of calculations were carried out to evaluate the response of the numerical model to controlled introduction of secondary fuel in the gutter section. Only phase of the fuel injection (relative to the phase of the pressure perturbation) was varied for this study. Figures 5a and 5b show respectively, the amplitude and the phase of the pressure perturbation at the chosen location for a range of phase delays. The results show that the amplitude of the pressure perturbation at the chosen location is sensitive to the phase delay with a minimum occurring near 165 degrees. This is a demonstration of the Rayleigh criterion which implies that (ideally) when the unsteady heat release and pressure perturbation are *out-of-phase*, (i.e., a phase delay of 180 degrees) the pressure amplitude is reduced.

## 4.3 Fuzzy Control Simulations

The open loop results were employed to devise the fuzzy rules. As noted earlier, these rules are developed using membership functions. For the present demonstration, the methodology described in section 3 has been simplified considerably (this is not necessary and will be refined in the future). The error between the sensor signal and the (pre-specified) value is defined as:

$$E_{\hat{p}} = \left[\left|\hat{p}_{sensor}\right| - \left|\hat{p}_{set}\right|\right] / \left|\hat{p}_{set}\right| \qquad (19)$$

where the subscripts *sensor* and *set* are respectively, the measured sensor amplitude and the pressure amplitude required to be achieved (and hence, pre-specified) at the chosen location. The goal of the controller is to minimize $E_{\hat{p}}$. The fuzzy set for the pressure amplitude is simplified to : {*large, medium, small* } and the membership functions for this set is shown in Figure 6. The y-axis in this figure denotes the probability of the set members and the x-axis denotes the error $E_{\hat{p}}$. For example, the membership function for *large* can be written as (see Fig. 6):

$$\Gamma(E_{\hat{p}}, 0.55, 0.70) = \begin{cases} 0 & E_{\hat{p}} < 0.55 \\ \left(E_{\hat{p}} - 0.55\right) \Big/ 0.15 & 0.55 \le E_{\hat{p}} \le 0.70 \\ 1 & E_{\hat{p}} > 0.70 \end{cases} \qquad (20)$$

where $\Gamma(a,b,c)$ is the membership function and the constants in the above expression are chosen by analyzing the open loop results. Similar functions are used for the other members of the sensor fuzzy set (see Fig. 6). The secondary fuel injection phase fuzzy set is defined as: {*big, medium, small*} and the membership functions for these set members are shown in Fig. 7. The values of the phase in Fig. 7 ($\Phi_s, \Phi_m, \Phi_b$) are determined based on the open loop results.

Once the membership functions are defined, the fuzzy rules must be specified. Again, a simplified version of the approach described in section 3 is employed for the present study. The fuzzy rules chosen for the present study are:

If $E_{\hat{p}}$ is large, then $\Phi_f$ is big
If $E_{\hat{p}}$ is medium, then $\Phi_f$ is medium
If $E_{\hat{p}}$ is small, then $\Phi_f$ is small

where $\Phi_f$ is the phase delay relative to the phase of the pressure perturbation at the sensor. Although, a general purpose controller will execute a weighted average of all the probabilities of occurrence of the above rules (see section 3), for the present demonstration, the rule with the largest probability was assumed to be the executed rule. This simplification (which is not necessary for the model) will be relaxed in future studies.

Figure 8 shows the flow chart of the implementation of the fuzzy controller with the reheat buzz device. As shown, the sensor signal is normalized and processed through the *fuzzification module* (which computed the probabilities using the membership functions, see Fig. 6). The logic rules are then used to obtain an appropriate response from the controller. This response is converted back to the physical space using *defuzzification* module (using the membership functions, see Fig. 7). The phase delay determined by this process is then used to modify the phase of the secondary fuel injection.

Figures 9a-9d show the result of the application of the fuzzy controller. For this simulation (using configuration 1), the goal was to achieve a pressure amplitude of $\left|\hat{p}/\hat{p}_{ref}\right| = 1$ at the location $x/L = 1.41$ (indicated by a solid symbol in the figure). At this location, without control, the amplitude was $\left|\hat{p}/\hat{p}_{ref}\right| = 1.375$. Based on the membership functions (see Fig. 6, 7), this set point was *within* the rule base. Thus, the controller was able to achieve acceptable control in the first attempt. As seen in Fig. 9b, the phase of the pressure perturbation is reversed (relative to the fuel phase, Fig. 9d). Furthermore, the amplitude of heat release fluctuation (Fig. 9c) is reduced when the control becomes effective.

Further studies showed that, as long as the control requirement was within the rule base, the controller was quite effective. However, when the set point is outside the rule base the controller had difficulty and in fact, actually failed to achieve the required goal. Figure 10a shows the pressure amplitude for a case when the goal was $\left|\hat{p}/\hat{p}_{ref}\right| = 0.5$ and demonstrates that even after two attempts the set point was not achieved. Therefore, the rule base was modified (by carrying out an additional open-loop control simulation) to include the new set point and the control was tried again. In this case, the control was successful, as shown in Figure 10b. This adaptation of the rule base was also automated recently thereby providing an adaptive capability that can be used to dynamically change the performance of the controller depending upon the set point.

The fuzzy controller was then applied to test conditions (similar to configuration 1) which was experimentally studied by Langhorne et al. (1989). Whereas in their study a deterministic feedback controller was used, in the present case, the fuzzy controller was used. Figure 11a shows the pressure amplitude (shown as the pressure band level (PBL), see Langhorne et al., 1989) in the combustor with and without control. The present results when compared with the experimental data clearly shows excellent agreement. Figure 11b shows the variation of the pressure amplitude with phase delay (shown in term of time delay and computed from the phase delay). Again, the results are in very good agreement with experimental data.

## 5. Conclusions

This paper has demonstrated a fuzzy logic based feedback controller to suppress combustion instability in a reheat buzz device. This device is a simplified approximation to an afterburner in an engine nozzle. Using a previously validated numerical model, a series of calculations were carried out to develop the expertise needed to devise the fuzzy logic rules. Subsequently, these rules were implemented into the reheat buzz model and the capability of the fuzzy controller was evaluated. The results clearly demonstrate that the fuzzy controller is as effective as deterministic controllers. When the control requirements are within the fuzzy rule base the controller achieves the required control at the first attempt. When the control requirement was outside the rule base, a simple redefinition of the rule base is sufficient to achieve control. Comparison with earlier experimental and numerical results clearly show that the present calculations agree quite well with data. The fact that the rule base was developed using only a few "training" runs suggests that this type of controller can be quickly brought into operation in actual devices. Furthermore, since the rule base is general, it is planned to study the response of this controller on a multi-dimensional dump combustor (where similar instability has been observed). This is an issue of current research and will be reported in the future.

## Acknowledgments

This work was supported by Office of Naval Research - SERDP Program under Grant No. N00014-95-1-0163 and is gratefully acknowledged.

## References


Bloxsidge, G. J., Dowling, A. P., Hooper, N., and Langhorne, P. J. (1987) "Active Control of an Acoustically Driven Combustion Instability," *J. Theo. and Appl. Mech.*, Vol. 6, pp. 161-175.

Bloxsidge, G. J., Dowling, A. P., and Langhorne, P. J. (1988a) "Reheat buzz: an acoustically coupled combustion instability. Part 2. Theory," *J. Fluid Mech.*, Vol. 193, pp. 445-473.

Bloxsidge, G. J., Dowling, A. P., Hooper, N. and Langhorne, P. J. (1988b) "Active control of reheat buzz," *AIAA J.*, Vol. 26, pp. 783-790.

Dowling, A. P. (1989) "Reheat Buzz - An Acoustically Coupled Combustion Instability," AGARD CP-450, Proceedings of the Propulsion and Energetics Panel, &2nd B Specialist Meeting, Bath, U.K.

Driankov, D., Hellendoorn, H. and Reinfrank, M. (1993) "An Introduction to Fuzzy Control," Springer-Verlag, Berlin.

Gutmark, E. and Wilson, K. J., Yu, K. H., and Schadow, K. C. (1995) "Active Control of a Liquid Fuel Dump/Bluff-Body Combustor Using Pulsed Fuel Injection," AIAA 95-0809.

Kim, S., Kumar, A., Dorrity, J. L. and Vachtsevanos, G. (1994) "Fuzzy Modeling, Control and Optimization of Textile Process," preprint.

Kosko, B. (1992) "Neural Networks and Fuzzy Systems", Englewood Cliffs, Prentice Hall.

Langhorne, P. J. (1988) "Reheat buzz: An acoustically coupled combustion instability. Part I. Experiments," *J. Fluid Mech.*, Vol. 193, pp. 417-443.

Langhorne, P. J. and Hooper, N. (1989) "Attenuation of reheat buzz by active control," AGARD CP-450.

Langhorne, P. J., Dowling, A. P., and Hooper, N. (1989) "A Practical Active Control System for Combustion Instability," *J. Prop. and Power*, Vol., 5.

Lang, W., Pointsot, T., and Candel, S. (1987) "Active control of combustion instability," *Comb. and Flame*, Vol. 70, pp. 281-289.

Menon, S., and Jou, W.-H., (1991)"Large-Eddy Simulations of Combustion Instability in an Axisymmetric Ramjet Combustor," *Combustion Sci. and Tech.*, Vol. 75, pp. 53-72.

Menon, S., (1992a) "A Numerical Study of Secondary Fuel Injection Technique for Active Control of Combustion Instability in a Ramjet," AIAA Paper No.92-0777.

Menon, S., (1992b) "Active Combustion Control in a Ramjet Using Large-Eddy Simulations," *Combustion Science and Technology*, Vol. 84, pp. 51-79.

Menon, S., (1995) "Secondary Fuel Injection Control of Combustion Instability in a Ramjet", *Combustion Science and Technology*, Vol. 100, pp. 385-393.

Ono, H., Ohnishi, T., and Terada, Y. (1989) "Combustion control of Refuse Incineration Plant by Fuzzy Logic," *Fuzzy Sets and Systems*, Vol. 32, pp. 193-206.

Poinsot, T. J., Trouve, A. C., Veynante, D.P., Candel, S. M., and Esposito, E.J. (1987a) "Vortex-Driven Acoustically Coupled Combustion Instability," *J. Fluid Mech.*, Vol. 177, pp. 265-292.

Poinsot, T. J., Bourienne, F., Esposito, E., Candel, S. M., and Lang, W. (1987b) "Suppression of Combustion Instability by Active Control," AIAA Paper No. 87-1876.

Schadow, K. C., Gutmark, E., Parr, T. P., Parr, D. M., Wilson, K.J ., and Crump, J. H. (1987) "Large-Scale Coherent Structures as Drivers of Combustion Instability," AIAA 87-1326.

Schadow, K. C., Gutmark, E., and Wilson, K. J. (1990) "Active Combustion Control in a Coaxial Dump Combustor," AIAA 90-2447.

Wilson, K. J., Gutmark, E., Schadow, K. C., and Smith, R. A. (1995) "Feedback Control of a Dump Combustor with Fuel Modulation," *J. Prop. and Power*, Vol. 11, No. 2.

Yu, K. H., Trouve, A., and Daily, J. W. (1991) "Low-Frequency Pressure Oscillations in a Model Ramjet Combustor," *J. Fluid Mech.*, Vol. 232, pp. 47-72.

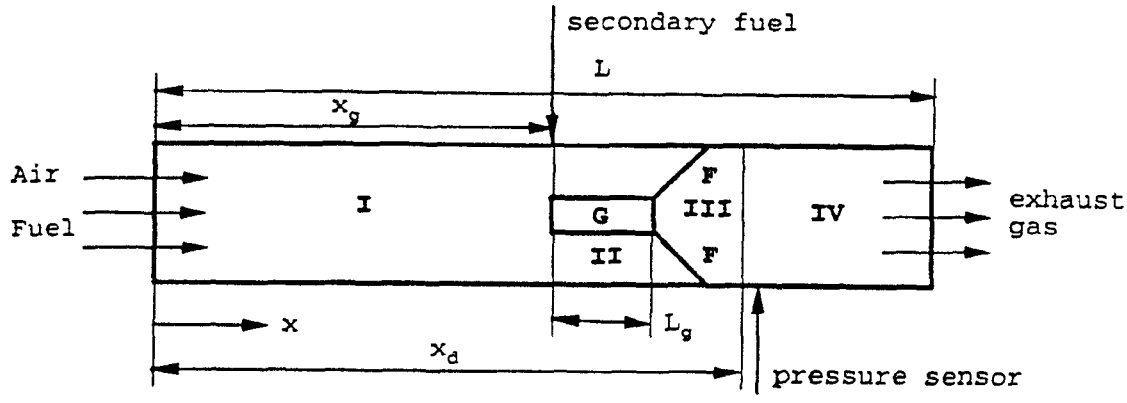


Figure 1. Schematic of the reheat buzz device. The symbol G indicates the gutter (flame holder) and F indicates the mean position of the flame.

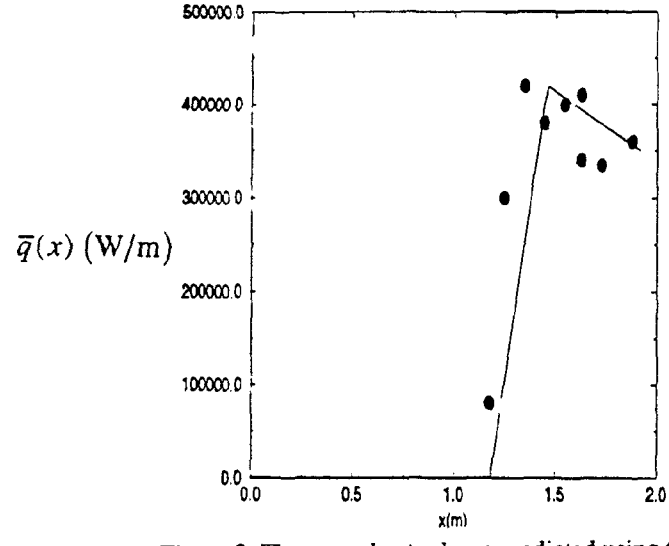


Figure 2. The mean heat release predicted using the established flame model. Solid symbols indicate the experimental data of Bloxsidge et al. (1988a).

| | Configuration 1 | Configuration 2 | Configuration 3 | Configuration 4 | Configuration 5 |
|---|---|---|---|---|---|
| Equivalence ratio | 0.70 | 0.65 | 0.66 | 0.65 | 0.71 |
| Inlet Mach Number | 0.08 | 0.08 | 0.08 | 0.08 | 0.15 |
| $x_g$(m) | 1.18 | 0.74 | 0.74 | 1.19 | 1.18 |
| L(m) | 1.92 | 1.48 | 1.48 | 2.18 | 1.92 |
| $x_{ref}$(m) | 0.75 | 0.49 | 0.49 | 0.75 | 0.75 |
| Flame Model | Established | Weak | Established | Established | Established |
| Experimental frequency, Langhore(1988) (Hz) | 77 | 81 | 103 | 77 | 109 |
| Frequency calculated by Dowling(1989) (Hz) | 81.6 | 78.3 | 102.8 | 81.2 | 110.1 |
| Growth rate calculated by Dowling(1989) (1/s) | -1.9 | -3.5 | -5.0 | -1.0 | 93.2 |
| Frequency calculated by Bloxsidge et al.(1988) (Hz) | 81.7 | 75.5 | 88.3 | 80.1 | 113.1 |
| Growth rate calculated by Bloxsidge et al.(1988) (1/s) | 1.1 | -4.4 | 68.1 | 33.1 | 86.6 |
| Frequency calculated by present study (Hz) | 78.0 | 76.1 | 102.5 | 80.6 | 105.0 |
| Growth rate calculated by present study (1/s) | -17.4 | -9.0 | 3.2 | 3.5 | -9.0 |

Table 1. Test conditions and predicted frequencies.

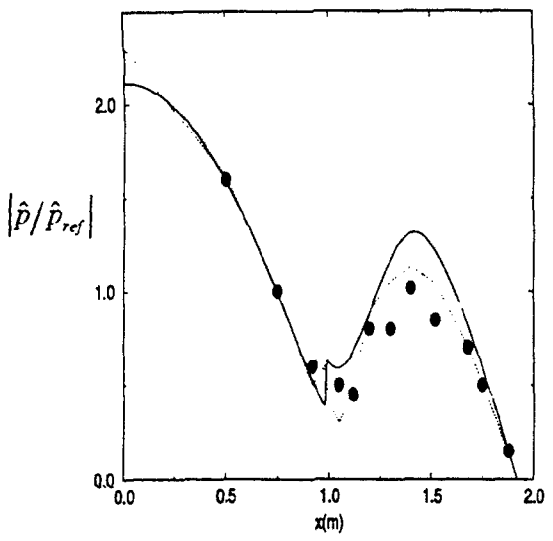


(a) The normalized pressure amplitude, $|\hat{p}/\hat{p}_{ref}|$.

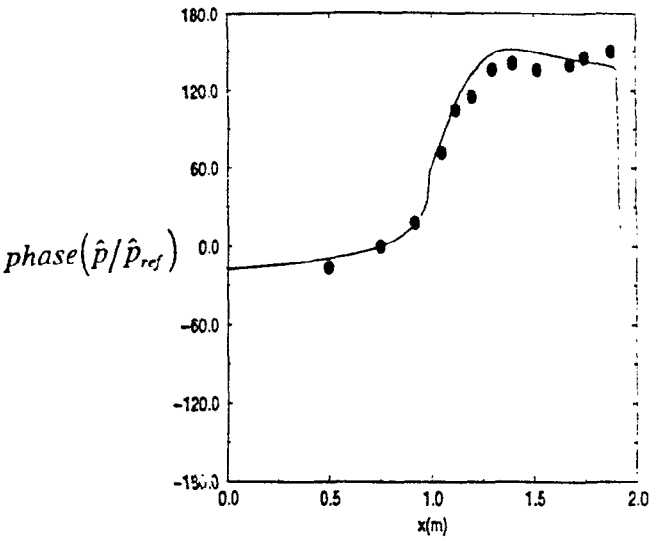


(b) The normalized pressure phase, $phase(\hat{p}/\hat{p}_{ref})$.

Figure 3. The pressure perturbation and phase for Configuration 1. Solid symbols: data from Bloxsidge et al. (1988a); Dotted curve: prediction by Bloxsidge et al. (1988a).

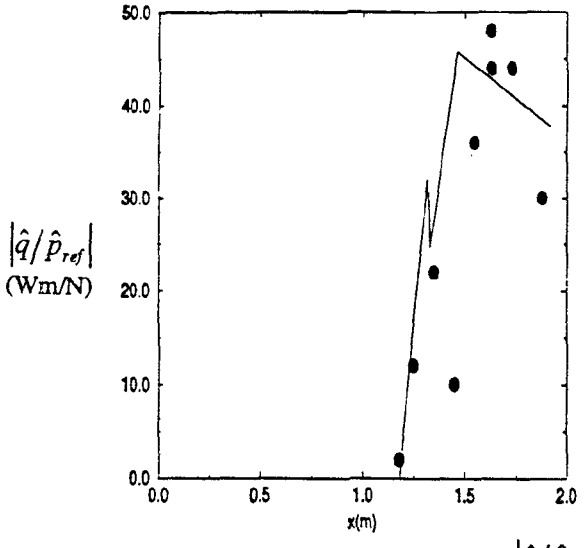


(a) The normalized heat release amplitude, $|\hat{q}/\hat{p}_{ref}|$.

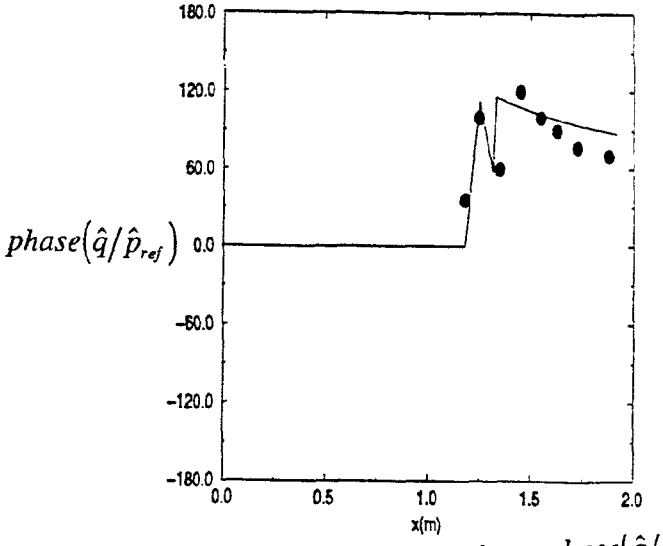


(b) The normalized heat release phase, $phase(\hat{q}/\hat{p}_{ref})$.

Figure 4. The heat release perturbation and phase for Configuration 1. Solid symbols: data from Bloxsidge et al. (1988a).

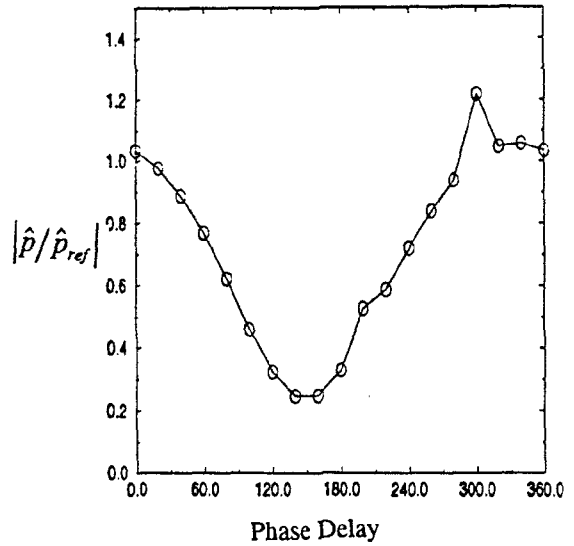


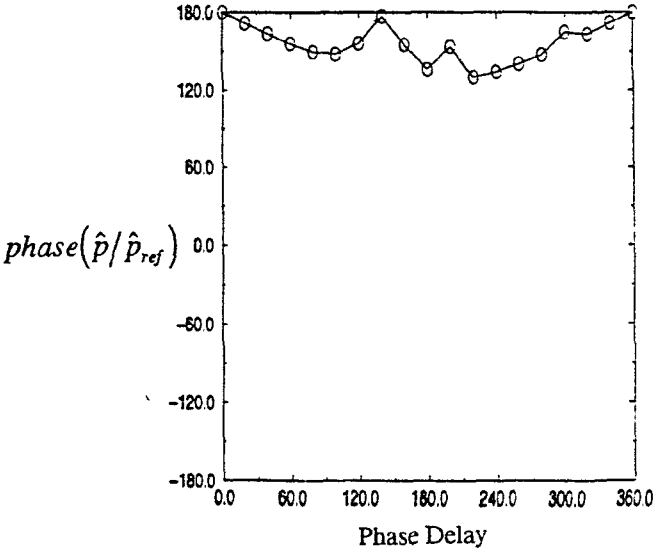


Figure 5. The pressure perturbation amplitude and phase measured at the sensor location for a range of phase delays of the secondary fuel injection. Open loop control simulations.

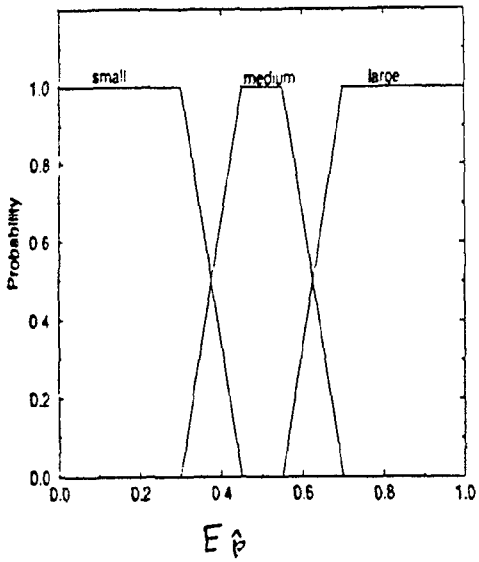


Figure 6. The membership functions for the pressure perturbation.

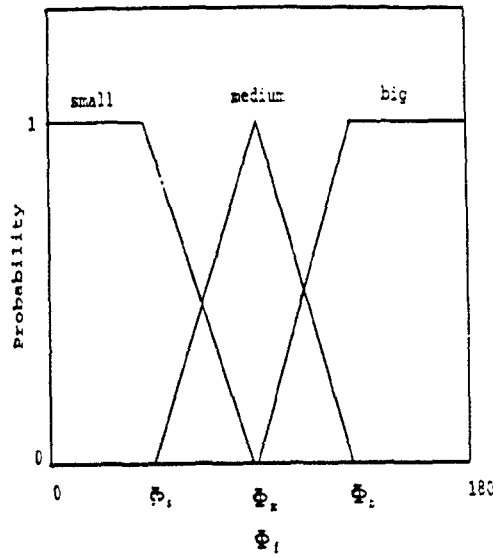


Figure 7. The membership functions for the unsteady fuel injection phase.

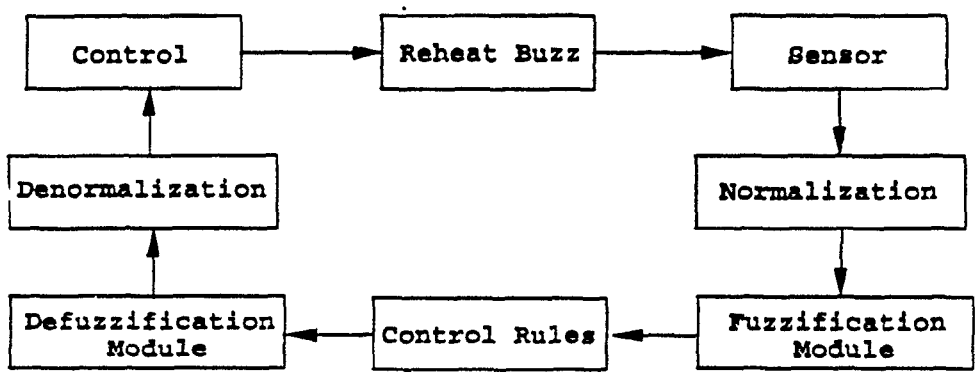


Figure 8. Schematic of the application of the fuzzy controller in the reheat buzz control.

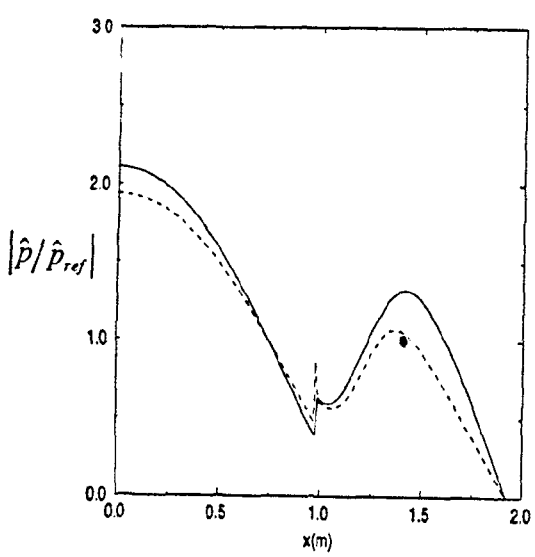


(a) The normalized pressure amplitude, $\left|\hat{p}/\hat{p}_{ref}\right|$.

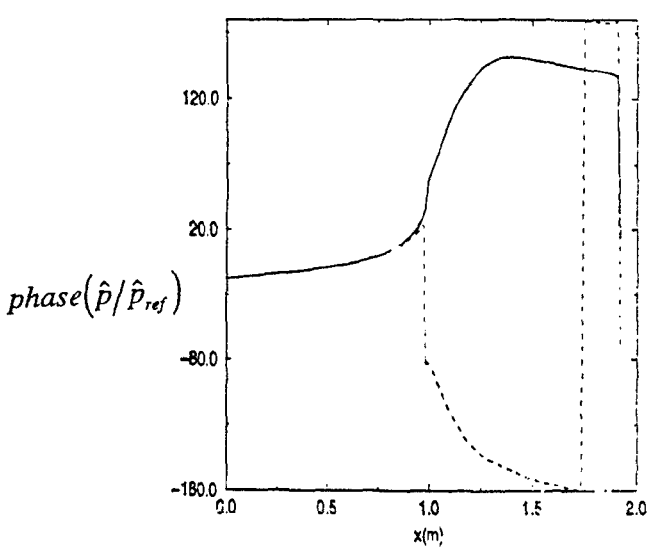


(b) The normalized pressure phase, $phase\left(\hat{p}/\hat{p}_{ref}\right)$.

Figure 9. Fuzzy control of reheat buzz when the set point is within the rule base. The solid symbol indicates the specified set point of $\left|\hat{p}/\hat{p}_{ref}\right|_{set} = 1.0$. The solid curve is the result without control and the dotted curve is the control prediction at the first attempt.

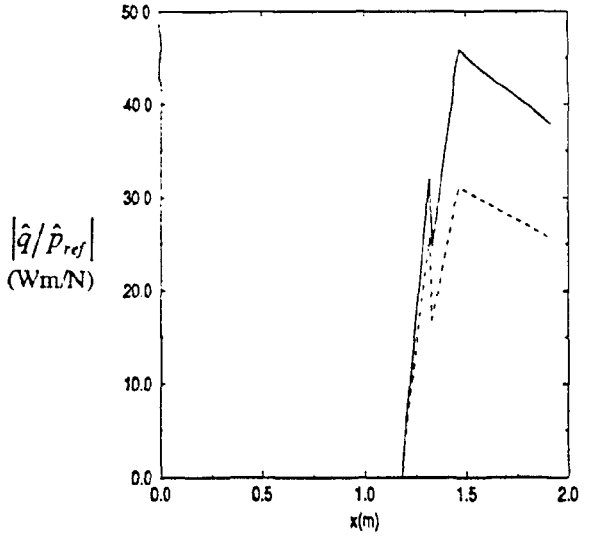


(c) The normalized heat release amplitude, $|\hat{q}/\hat{P}_{ref}|$.

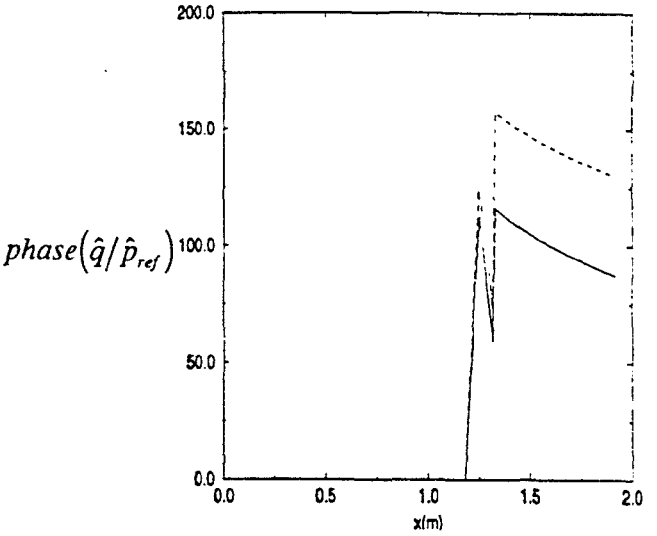


(d) The normalized heat release phase, $phase(\hat{q}/\hat{P}_{ref})$.

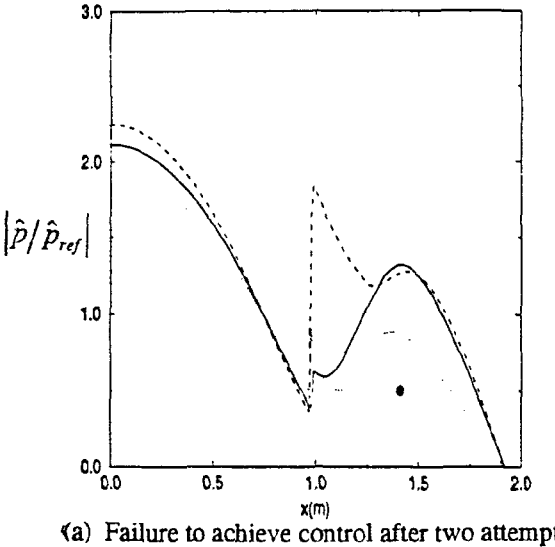


(a) Failure to achieve control after two attempts,

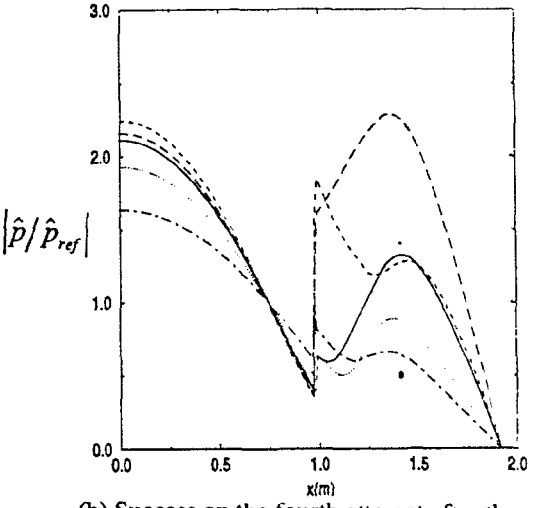


(b) Success on the fourth attempt after the rule base was modified.

Figure 10. The normalized pressure perturbation amplitude with fuzzy control. The set point was $|\hat{p}/\hat{P}_{ref}|_{set} = 0.5$ (shown as a solid symbol) which was outside the rule base specified earlier.

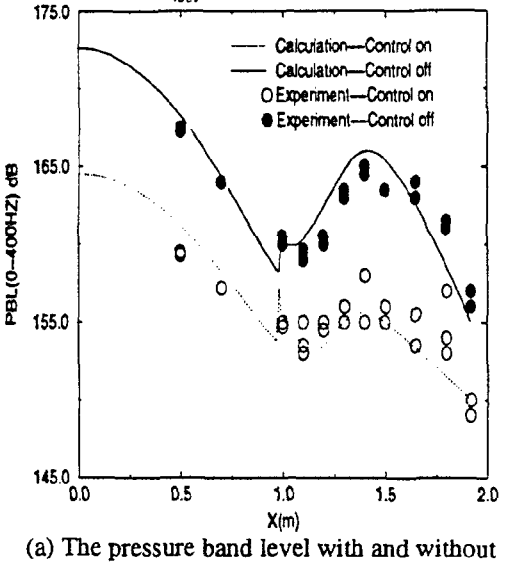


(a) The pressure band level with and without control as a function of axial distance.

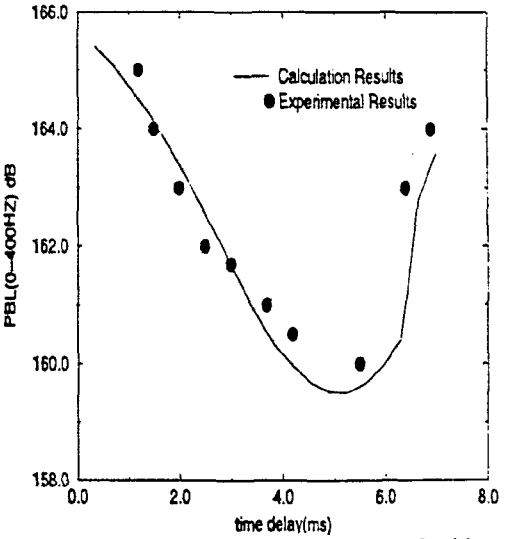


(b) The pressure band level with and without control as a function of time delay.

Figure 11. Comparison of predicted pressure band level (PBL) and time delay for control with experimental data of Langhorne et al. (1989). The experimental data with control was obtained using a deterministic feedback controller using secondary fuel injection.